Inorganic Chemistry

Article

pubs.acs.org/IC

Tetranuclear Hetero-Metal $[Co^{II}_2Ln^{III}_2]$ (Ln = Gd, Tb, Dy, Ho, La) Complexes Involving Carboxylato Bridges in a Rare $\mu_4-\eta^2:\eta^2$ Mode: Synthesis, Crystal Structures, and Magnetic Properties

Sk Md Towsif Abtab,[†] Mithun Chandra Majee,[†] Manoranjan Maity,[†] Ján Titiš,[‡] Roman Boča,*[,‡] and Muktimoy Chaudhury*[,†]

[†]Department of Inorganic Chemistry, Indian Association for the Cultivation of Science, Jadavpur, Kolkata 700 032, India

[‡]Department of Chemistry, FPV, University of SS Cyril and Methodius, 917 01 Trnava, Slovakia

Supporting Information

ABSTRACT: A new family of 3d−4f heterometal 2 × 2 complexes $[Co^{II}_2(L)_2(PhCOO)_2Ln^{III}_2(hfac)_4]$ (**1**−**5**) (Ln = Gd (compound **1**), Tb (compound **2**), Dy (compound **3**), Ho (compound **4**), and La (compound **5**)) have been synthesized in moderate yields (48−63%) following a single-pot protocol using stoichiometric amounts (1:1 mol ratio) of $[Co^{II}(H_2L)(PhCOO)_2]$ (H_2L = *N*,*N*′-dimethyl-*N*,*N*′-bis(2-hydroxy-3,5-dimethylbenzyl)ethylenediamine) as a metalloligand and $[Ln^{III}(hfac)_3(H_2O)_2]$ (Hhfac = hexafluoroacetylacetone) as a lanthanide precursor compound. Also reported with this series is the Zn−Dy analog $[Zn^{II}_2(L)_2(PhCOO)_2Dy^{III}_2(hfac)_4]$ **6** to help us in understanding the magnetic properties of these compounds. The compounds **1**−**6** are isostructural. Both hexafluoroacetylacetonate and benzoate play crucial roles in these structures as coligands in generating a tetranuclear core of high thermodynamic stability through a self-assembly process. The metal centers are arranged alternately at the four corners of this rhombic core, and the carboxylato oxygen atoms of each benzoate moiety bind all of the four metal centers of this core in a rare $\mu_4-\eta^2:\eta^2$ bridging mode as confirmed by X-ray crystallography. The magnetic susceptibility and magnetization data confirm a paramagnetic behavior, and no remnant magnetization exists in any of these compounds at vanishing magnetic field. The metal centers are coupled in an antiferromagnetic manner in these compounds. The $[Co^{II}_2Dy^{III}_2]$ compound exhibits a slow magnetic relaxation below 6 K, as proven by the AC susceptibility measurements; the activation energy reads U/k_B = 8.8 K ($\tau_0 = 2.0 \times 10^{-7}$ s) at $\mathbf{B}_{DC}$ = 0, and U/k_B = 7.8 K ($\tau_0 = 3.9 \times 10^{-7}$ s) at $\mathbf{B}_{DC}$ = 0.1 T. The $[Zn^{II}_2Dy^{III}_2]$ compound also behaves as a single-molecule magnet with U/k_B = 47.9 K and $\tau_0 = 2.75 \times 10^{-7}$ s.

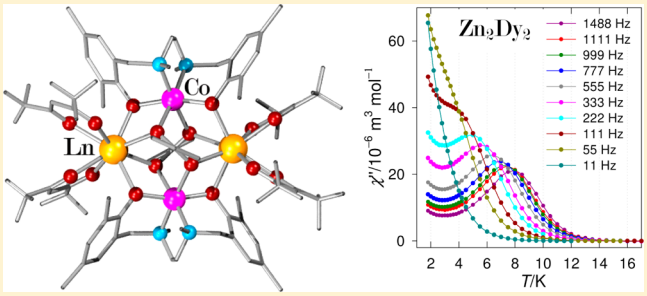

INTRODUCTION

The study of heterometal complexes containing 3d−4f metal ion combinations is an active area of research in contemporary coordination chemistry.[1] The initial interest in this field originated from a classic paper reported by Gatteschi et al.[2] on the ferromagnetic interaction between copper(II) and isotropic gadolinium(III) ion within a discrete trinuclear complex. The discovery of lanthanide-based single-molecule magnets (SMMs) is an important step forward[3] that includes 3d−4f compounds of certain lanthanide ions (Tb^{3+}, Dy^{3+}, Ho^{3+}, etc.) with large spin ground states (S_T) and exhibit strong magnetic anisotropy. Some of the resulting compounds find possible applications in the areas of information storage, molecular spintronics, quantum computation, magnetically addressable liquid crystals, magnetic alloys for refrigeration, etc.[4]

Interestingly, only a handful of such complexes with interesting magnetic properties have been reported thus far because of the inherent difficulties encountered during their preparation, mainly due to product scrambling. Most of these reported complexes are based on copper(II),[5] manganese(II),[6] and iron(III)[7] ions which can bring in, along with the lanthanide ions, larger ground state and stronger anisotropy in the resulting compounds. Surprisingly, however, there are very few examples of 3d−4f compounds involving cobalt(II) ion[8] in spite of their Ising-type magnetic anisotropy that supports SMM behavior.

We have recently reported[9a] the syntheses and structural characterization of carboxylato complexes $[M(H_2L)(PhCOO)_2]$ (M = Ni^{II} and Co^{II}) involving a tetradentate phenol-based pro-ligand H_2L. The nickel analogue of this pair has been used as a metalloligand for the successful synthesis of a family of tetra- and dinuclear nickel(II)−vanadium(IV/V) heterometal complexes.[9b] Herein, we report the synthesis of a new series of tetranuclear 2 × 2 heterometal complexes $[Co^{II}_2(L)_2(PhCOO)_2Ln^{III}_2(hfac)_4]$ (**1**−**5**) of cobalt(II) and lanthanide(III) ions (Ln = Gd, Tb, Dy, Ho, La), using

Received: June 12, 2013
Published: January 17, 2014

   dx.doi.org/10.1021/ic401484d | *Inorg. Chem.* 2014, 53, 1295−1306

Table 1. Summary of X-ray Crystallographic Data for Complexes 1−6

parameters	1	2	3	4	5	6
composition	$C_{78}H_{74}Co_2F_{24}Gd_2N_4O_{16}$	$C_{78}H_{74}Co_2F_{24}N_4O_{16}Tb_2$	$C_{78}H_{74}Co_2Dy_2F_{24}N_4O_{16}$	$C_{78}H_{74}Co_2F_{24}Ho_2N_4O_{16}$	$C_{78}H_{74}Co_2F_{24}La_2N_4O_{16}$	$C_{78}H_{74}Dy_2F_{24}N_4O_{16}Zn_2$
formula wt.	2211.77	2215.11	2222.27	2227.13	2175.09	2235.15
crystal system	monoclinic	monoclinic	monoclinic	monoclinic	orthorhombic	monoclinic
space group	*Cc*	*Cc*	*Cc*	*Cc*	$Pna2_1$	*Cc*
a, Å	12.487(4)	12.4119(9)	12.4052(5)	12.4729(8)	24.0316(13)	12.4944(7)
b, Å	30.961(11)	30.895(2)	30.8506(13)	31.218(2)	12.4015(7)	31.2598(17)
c, Å	23.215(7)	23.1418(16)	23.1455(10)	23.1884(15)	29.9633(16)	23.2190(12)
α, deg	90.00	90.00	90.00	90.00	90.00	90.00
β, deg	101.066(5)	100.714(3)	100.866(2)	100.334(2)	90.00	100.1840(10)
γ, deg	90.00	90.00	90.00	90.00	90.00	90.00
V, Å^3	8808(5)	8719.3(11)	8699.1(6)	8882.6(10)	8929.9(8)	8925.8(8)
ρ_{calc}, Mg m^{-3}	1.668	1.687	1.697	1.665	1.618	1.663
temp, K	100(2)	150(2)	150(2)	298(2)	298(2)	298(2)
λ (Mo K$_\alpha$), Å	0.71073	0.71073	0.71073	0.71073	0.71073	0.71073
Z	4	4	4	4	4	4
$F(000)/\mu$ mm^{-1}	4384/1.971	4392/2.092	4400/2.189	4408/2.242	4328/1.415	4424/2.299
$2\theta_{max}$ [^{o}]	55.80	45.28	50.94	49.10	42.16	48.58
reflections collected/unique	15080/13271	10700/9153	14797/12451	14227/11400	9565/8401	12765/10374
R_{int}/ GOF on F^2	0.0278/1.136	0.0700/1.084	0.0484/0.853	0.0430/0.905	0.0579/1.129	0.0514/0.864
number of parameters	1147	1147	1147	1147	1142	1147
$R1^a(F_0)$, $wR2^b(F_0)$	0.0441	0.0711	0.0556	0.0613	0.0455	0.0575
(all data)	0.0828	0.1529	0.1236	0.1349	0.0872	0.1252
largest diff. peak, deepest hole, eÅ^{-3}	0.884, −0.542	1.671, −1.528	0.738, −0.530	0.717, −0.357	0.443, −0.309	0.695, −0.383

$^aR = \sum||F_o| - |F_c||/\sum|F_o|$. $^bwR = [\sum[w((F_o^2 - F_c^2)^2]/\sum w(F_o^2)^2]^{1/2}$.

$[Co^{II}(H_2L)(PhCOO)_2]$ (H_2L = *N*,*N*′-dimethyl-*N*,*N*′-bis(2-hydroxy-3,5-dimethylbenzyl)-ethylenediamine) as a metalloligand and $[Ln^{III}(hfac)_3(H_2O)_2]$ (Hhfac = hexafluoroacetylacetone) as a lanthanide precursor. Also reported along with this series is a $Zn^{II}_2Dy^{III}_2$ compound $[Zn^{II}_2(L)_2(PhCOO)_2Dy^{III}_2(hfac)_4]$ (**6**) that will help in understanding the magnetic properties of complexes **1**−**5**. The compounds have been characterized by single-crystal X-ray diffraction analysis. Their magnetic properties have been investigated in detail.

EXPERIMENTAL SECTION

Materials. All reactions were carried out in an aerobic environment with commercially available chemicals that were used as received. The precursor complexes $[Ln^{III}(hfac)_3(H_2O)_2]$[10] (Ln = Gd, Tb, Dy, Ho, La) and $[Co^{II}(H_2L)(PhCOO)_2]$[9a] were prepared following reported methods. Solvents were reagent grade, dried by standard methods,[11] and distilled under nitrogen prior to their use.

Preparation of Compounds. $[Co^{II}_2(L)_2(PhCOO)_2Gd^{III}_2(hfac)_4]$ 1. To a stirred solution containing $[Gd^{III}(hfac)_3(H_2O)_2]$ (0.82 g, 1 mmol) in 50 mL of ethanol was added $[Co^{II}(H_2L)(PhCOO)_2]$ (0.65 g, 1 mmol). The resulting solution was refluxed for 6 h during which time a light orange solution was obtained. It was then kept in the open air for slow evaporation. Block-shaped orange-brown crystals were obtained within 4−5 d. Some of these crystals were of diffraction quality and were used directly for X-ray structure analysis. Yield: 0.64 g (58%). Anal. Calcd for $C_{78}H_{74}Co_2F_{24}Gd_2N_4O_{16}$: C, 42.36; H, 3.37; N, 2.53. Found: C, 42.19; H, 3.24; N, 2.63%. Fourier transform infrared (FT-IR) bands (KBr pellet, cm^{-1}): 2923, 2867, 1664, 1593, 1554, 1514 1477, 1394, 1315, 1257, 1211, 1145, 1101, 860, 796, 730, 661, 584.

$[Co^{II}_2(L)_2(PhCOO)_2Tb^{III}_2(hfac)_4]$ 2. This compound was obtained as an orange-brown crystalline product by following a procedure as described above for compound **1**, using $[Tb^{III}(hfac)_3(H_2O)_2]$ as a replacement for $[Gd^{III}(hfac)_3(H_2O)_2]$. The orange solution obtained after reflux was filtered. The filtrate was left in the air for slow evaporation. The dark orange crystalline product was obtained after ca. 5 d. Some of these crystals were of diffraction grade and used directly for crystal structure analysis. Yield: 0.70 g (63%). Anal. Calcd for $C_{78}H_{74}Co_2F_{24}N_4O_{16}Tb_2$: C, 42.29; H, 3.37; N, 2.53. Found: C, 42.42; H, 3.31; N, 2.61%. FT-IR bands (KBr pellet, cm^{-1}): 2923, 2868, 1656, 1593, 1554, 1515 1477, 1392, 1313, 1255, 1209, 1147, 1095, 860, 796, 731, 656, 582.

$[Co^{II}_2(L)_2(PhCOO)_2Dy^{III}_2(hfac)_4]$ 3. This compound was prepared by following a similar method as described above for complex **1**, using $[Dy^{III}(hfac)_3(H_2O)_2]$ as a replacement for $[Gd^{III}(hfac)_3(H_2O)_2]$. Orange-brown single crystals suitable for X-ray crystal structure analysis, formed at room temperature by slow evaporation of the filtrate over a period of 4 d, were collected by filtration. Yield: 0.60 g (54%). Anal. Calcd for $C_{78}H_{74}Co_2Dy_2F_{24}N_4O_{16}$: C, 42.16; H, 3.36; N, 2.52. Found: C, 42.28; H, 3.28; N, 2.59%. FT-IR bands (KBr pellet, cm^{-1}): 2923, 2867, 1658, 1595, 1554, 1514, 1477, 1393, 1314, 1255, 1207, 1145, 1097, 860, 796, 731, 655, 584.

$[Co^{II}_2(L)_2(PhCOO)_2Ho^{III}_2(hfac)_4]$ 4. This compound was prepared as orange-brown crystals by following the procedure described above for complex **1** but using $[Ho^{III}(hfac)_3(H_2O)_2]$ instead of $[Gd^{III}(hfac)_3(H_2O)_2]$. Crystals suitable for X-ray structure analysis were obtained by slow evaporation of an ethanolic solution of the compound. Yield: 0.66 g (59%). Anal. Calcd for $C_{78}H_{74}Co_2F_{24}Ho_2N_4O_{16}$: C, 42.06; H, 3.35; N, 2.52. Found: C, 41.94; H, 3.28; N, 2.46%. FT-IR bands (KBr pellet, cm^{-1}): 2921, 2862, 1650, 1595, 1552, 1527, 1475, 1396, 1309, 1255, 1205, 1146, 1101, 860, 796, 727, 667, 584.

$[Co^{II}_2(L)_2(PhCOO)_2La^{III}_2(hfac)_4]$ 5. This compound was prepared by following the same procedure as described above for complex **1**, using $[La^{III}(hfac)_3(H_2O)_2]$ as a replacement for $[Gd^{III}(hfac)_3(H_2O)_2]$. Orange-brown single crystals suitable for X-ray crystal structure analysis were formed at room temperature by slow evaporation of the filtrate over a period of 4 d and were collected by filtration. Yield: 0.52 g (48%). Anal. Calcd for $C_{78}H_{74}Co_2F_{24}La_2N_4O_{16}$: C, 43.05; H, 3.43; N, 2.58. Found: C, 42.92; H, 3.36; N, 2.53%. FT-IR bands (KBr pellet, cm^{-1}): 2923, 2867, 1656, 1593, 1554, 1515, 1477, 1440, 1392, 1313, 1255, 1207, 1147, 1095, 1002, 860, 796, 731, 659, 582.

$[Zn^{II}_2(L)_2(PhCOO)_2Dy^{III}_2(hfac)_4]$ 6. $Zn^{II}(ClO_4)_2{\cdot}6H_2O$ (0.37 g, 1 mmol) and H_2L (0.36 g, 1 mmol) and sodium benzoate (0.29 g, 2 mmol) were dissolved in 50 mL of EtOH and stirred for 30 min. To

dx.doi.org/10.1021/ic401484d | Inorg. Chem. 2014, 53, 1295−1306

the resulting clear solution, solid $[Dy^{III}(hfac)_3(H_2O)_2]$ (0.82 g, 1 mmol) was added; this solution was refluxed for 6 h to get a light yellow solution. It was filtered, and the filtrate was left in the air for slow evaporation to get the pale yellow crystalline product in about 5 d. Yield: 0.67 g (60%). Anal. Calcd for $C_{78}H_{74}Dy_2F_{24}N_4O_{16}Zn_2$: C, 41.89; H, 3.34; N, 2.51. Found: C, 41.77; H, 3.30; N, 2.44%. FT-IR bands (KBr pellet, cm^{-1}): 2923, 2867, 1662, 1595, 1554, 1523, 1477, 1392, 1315, 1257, 1213, 1145, 1101, 860, 792, 731, 663, 584.

Physical Measurements. Elemental analyses for C, H, and N were performed at IACS on a Perkin-Elmer model 2400 Series II CHNS Analyzer. The IR spectra of the samples prepared as KBr pellets were recorded using a Shimadzu model 8400S FT-IR spectrometer.

The magnetic data were taken with the SQUID apparatus (MPMS-XL7, Quantum Design) using the Reciprocating Sample Option mode of detection with ca. 6 mg of the sample encapsulated in a gelatin-made sample holder. The susceptibility taken at **B** = 0.1 T has been corrected for the underlying diamagnetism. The magnetization was measured at two temperatures: T = 2.0 and 4.6 K. The magnetization data were taken in the field-decreasing mode to eventually catch the remnant magnetization. The AC susceptibility measurements at different frequencies between ν = 11−1512 Hz were conducted at a working field of $\mathbf{B}_{AC}$ = 0.38 mT and an eventual applied field of $\mathbf{B}_{DC}$ = 0.1 T. Twenty scans were averaged for each measurement.

X-ray Crystallography. Suitable crystals of complex **1** (orange-brown block, 0.22 × 0.16 × 0.16 mm^3), complex **2** (orange-brown block, 0.20 × 0.18 × 0.14 mm^3), complex **3** (orange-brown block, 0.22 × 0.16 × 0.12 mm^3), complex **4** (orange-brown block, 0.20 × 0.17 × 0.14 mm^3), complex **5** (orange-brown block, 0.18 × 0.15 × 0.12 mm^3), and complex **6** (pale yellow block, 0.24 × 0.21 × 0.17 mm^3) were collected following the procedure as described above in the synthesis part and mounted on glass fibers. Intensity data for the compounds were measured employing a Bruker SMART APEX II CCD diffractometer equipped with a monochromatized Mo K_α radiation (λ = 0.71073 Å) source at 100(2) K for complex **1**, 150(2) K for complexes **2** and **3**, and 298(2) K for complexes **4**, **5**, and **6**. No crystal decay was observed during the data collections. The intensity data were corrected for empirical absorption. In all cases, absorption corrections based on multiscan using the SADABS software[12] were applied.

The structures were solved by direct methods[13] and refined on F^2 by a full-matrix least-squares procedure[13] based on all data minimizing $R = \sum ||F_0| - |F_c||/\sum|F_0|$, $wR = [\sum[w(F_0^2 - F_c^2)^2]/\sum(F_0^2)^2]^{1/2}$, and $S = [\sum[w(F_0^2 - F_c^2)^2]/(n - p)]^{1/2}$. SHELXL-97 was used for both structure solutions and refinements.[14] A summary of the relevant crystallographic data and the final refinement details are given in Table 1. All non-hydrogen atoms were refined anisotropically. The hydrogen atoms were calculated and isotropically fixed in the final refinement [d(C−H) = 0.95 Å, with the isotropic thermal parameter of U_{iso}(H) = 1.2 U_{iso}(C)]. The SMART and SAINT software packages[15] were used for data collection and reduction, respectively. Crystallographic diagrams were drawn using the DIAMOND software package.[16]

RESULTS AND DISCUSSION

Syntheses. The heterometallic tetranuclear complexes of general formula $[Co^{II}_2(L)_2(PhCOO)_2Ln^{III}_2(hfac)_4]$ (Ln = Gd, Tb, Dy, Ho, La) have been synthesized in moderate yields (48−63%) as crystalline solids by the self-assembly reaction involving stoichiometric amounts (1:1 mol ratio) of $[Co^{II}(H_2L)(PhCOO)_2]$ and $[Ln^{III}(hfac)_3(H_2O)_2]$ [Ln = Gd (complex **1**), Tb (complex **2**), Dy (complex **3**), Ho (complex **4**), La (complex **5**)] in ethanol under refluxing conditions, as summarized in Scheme 1. The precursor compound $[Co^{II}(H_2L)(PhCOO)_2]$ in this protocol functions as a metalloligand, and $[Ln^{III}(hfac)_3(H_2O)_2]$ functions as an acceptor having substitutable coordination sites. Also reported is the $Zn^{II}_2Dy^{III}_2$ compound $[Zn^{II}_2(L)_2(PhCOO)_2Dy^{III}_2(hfac)_4]$ **6**, prepared by an analogous procedure in which the zinc(II) ion is used to substitute for the cobalt(II) centers. The high thermodynamic stability of this self-assembled tetranuclear core is possibly the driving force here that directs each carboxylato group to bridge all the four metal centers in a rare μ_4−η^2:η^2-type mode[17] as confirmed by X-ray diffraction analyses (see later discussion).

Scheme 1. Protocol Followed for the Synthesis of Complexes 1−6

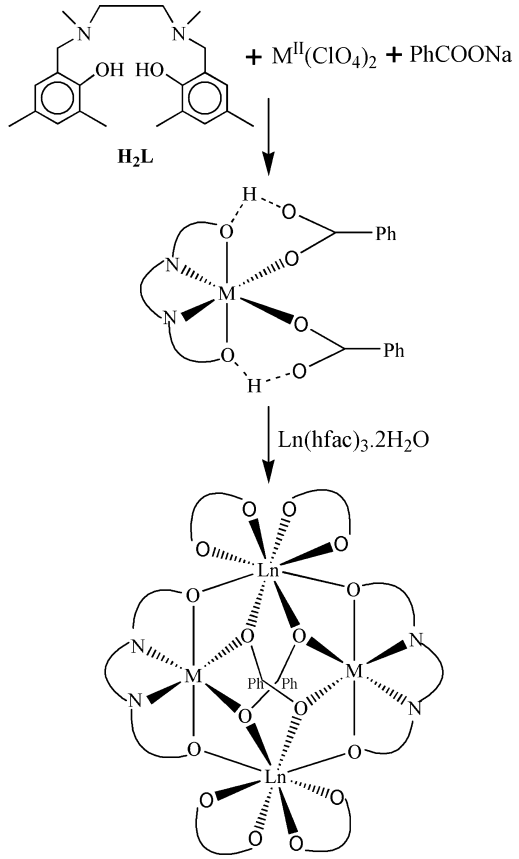

	1	2	3	4	5	6
M =	Co	Co	Co	Co	Co	Zn
Ln =	Gd	Tb	Dy	Ho	La	Dy

The IR spectra of complexes **1**−**6** show all the characteristic bands for the coordinated tetradentate ligand $(L)^{2-}$. One such prominent band appears at ca. 1255 cm^{-1} due to ν(C−O/phenolate) stretching. Of particular interest here is the appearance of strong bands in the region of 1514−1554 cm^{-1} and at ca. 1392 cm^{-1} due to $\nu_{asym}(COO^-)$ and $\nu_{sym}(COO^-)$ vibrations, respectively of the ancillary carboxylato ligand.[18] Corresponding signature vibrations for the β-diketonate moiety appear at ca. 1660 cm^{-1} due to ν(C═O) and at ca. 1145 and 1210 cm^{-1} due to ν(C−F) stretching modes.[19]

Description of Crystal Structures. The heterometal complexes are all isostructural with four molecular weight units accommodated in their respective unit cell. Identical atom-labeling schemes have been adopted for all the structures for easy comparison of their relevant metrical parameters (Table S1, Supporting Information). The structure of complex **1**, which crystallizes in the monoclinic space group Cc, is described here as a representative example of this series involving $Co^{II}_2Ln^{III}_2$ metal combinations (complexes **1**−**4**). A perspective view of complex **1** is depicted in Figure 1. The

dx.doi.org/10.1021/ic401484d | Inorg. Chem. 2014, 53, 1295−1306

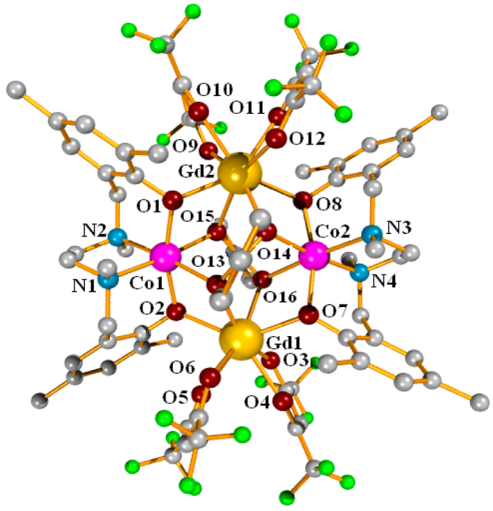

Figure 1. Partially labeled POV-Ray (in ball and stick form) diagram showing the atom-labeling scheme for the complex **1**.

asymmetric unit consists of a neutral tetranuclear $[Co^{II}_2(L)_2(PhCOO)_2Gd^{III}_2(hfac)_4]$ core in which the cobalt(II) and gadolinium(III) ions are arrayed alternately at the corners of a rectangular plane. The cobalt(II) centers in this core have distorted octahedral geometry involving N_2O_4 donor sets, while the larger and harder gadolinium(III) ions take up the eight coordination sites involving all oxygen O_8 donor combinations. The octahedral geometry around Co(1) and Co(2) centers are completed by the O(1), N(1), N(2), and O(2) [O(7), N(3), N(4), and O(8) for Co(2)] donor atoms, all coming from the tetradentate ligand $(L)^{2-}$, together with O(13) and O(15) atoms [O(14) and O(16)] from the two bridging benzoate ligands. At the Co(1) center, the benzoato oxygen atoms O(13) and O(15) [O(14) and O(16) for Co(2)] along with the amino nitrogen atoms N(2) and N(1) [N(3) and N(4)] form the N_2O_2 basal plane, while the apical positions are taken up by the phenolate oxygen atoms O(1) and O(2) [O(7) and O(8)]. The trans angles of N(1)–Co(1)–O(15) 175.15(18)°, N(2)–Co(1)–O(13) 175.17(18)°, N(3)–Co(2)–O(16) 175.21(16)°, and N(4)–Co(2)–O(14) 174.88(17)° are close to linearity, while the remaining two angles, O(1)–Co(1)–O(2) 164.22(17)° and O(7)–Co(2)–O(8) 165.12(15)°, are well short of the target, because of the restrictions imposed by the bridging phenolate oxygen atoms O(1), O(2), O(7), and O(8). Of the eight oxygen donor atoms surrounding a Gd(1) center, four are bridging oxygen atoms, namely, O(2), O(7), O(13), and O(16) [O(1), O(8), O(14), and O(15) for Gd(2)] playing a crucial role in binding the metal centers, both Co^{II} and Gd^{III}, together to form a crown (Figure S1, Supporting Information). The first two of these are phenolate oxygen atoms, coming from two tetradentate N_2O_2 ligands, each attached to an adjacent Co^{II} center, while the other two are from two carboxylates, which are in a rare μ_4–η^2:η^2-type bridging mode, one above and the other below the metal-containing plane (the rectangular plane connecting the four metal centers). Interestingly, while the phenoxo oxygen O(2) that bridges Co(1) and Gd(1) is lying above the metal plane, the carboxylate oxygen O(13) between the same two metal centers is lying below that plane. The bridging pattern is just reversed between the next immediate pair of metal centers [Co(1) and Gd(2)], thus generating an undulatory pattern of an octagonal crown (Figure S1, Supporting Information). The remaining four oxygen donors around the Gd^{III} centers are contributed by a pair of chelating $hfac^-$ ligands. This donor atom combination generates a bicapped pseudotrigonal prismatic coordination environment around both the Gd(1) and the Gd(2) centers, as shown in Figure 2. The Co···Gd separations are in the range of 3.593–

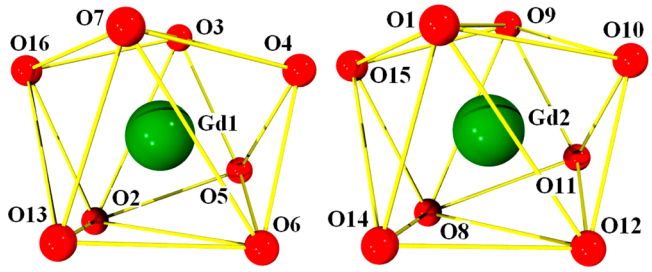

Figure 2. Bicapped pseudotrigonal prismatic coordination spheres around Gd(1) and Gd(2) in complex **1**.

3.623 Å, while the Co···Gd···Co (~80°) and Gd···Co···Gd (~100°) angles are complementary to each other, indicating a rhombic shape of the metal-containing plane in these heterometal complexes. Perspective views of the compounds **2**, **3**, and **4** are displayed (Figures S2–4, respectively, in the Supporting Information). Their relevant metrical parameters are summarized in Table S1.

The $Co^{II}_2La^{III}_2$ compound (**5**) is orthorhombic, with the space group $Pna2_1$, and has four molecular mass units accommodated per unit cell. Its molecular structure (Figure 3) is essentially the same as that of the other complexes of this

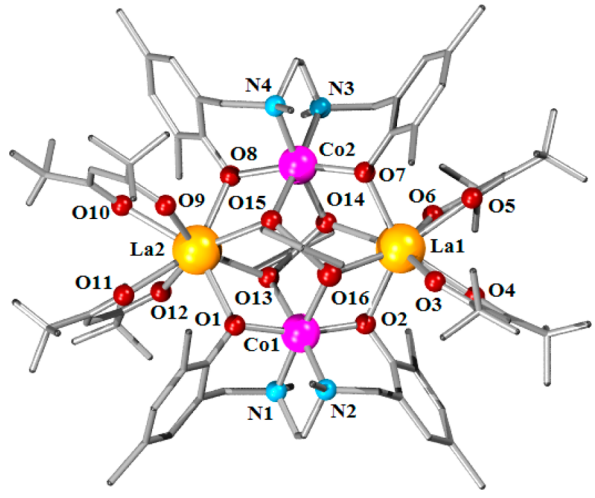

Figure 3. Partially labeled POV-Ray (in ball and stick form) diagram showing the atom-labeling scheme for the complex **5**.

series, with marginal differences in the La–O and La–N bond distances (Table S1, Supporting Information), which are due to the larger size of the La^{3+} ion. With Co centers in distorted octahedral and La centers with eight-coordinated bicapped pseudotrigonal prismatic geometry, this structure shows minimal differences, with Co···La separations in the range of 3.678–3.724 Å, and the Co···La···Co (~79°) and La···Co···La (~101°) angles are complementary to each other.

The perspective view of the molecular structure of $[Zn^{II}_2(L)_2(PhCOO)_2Dy^{III}_2(hfac)_4]$ **6** is shown in Figure 4. It may be noted that the replacement of Co^{II} by Zn^{II} has only a

dx.doi.org/10.1021/ic401484d | Inorg. Chem. 2014, 53, 1295–1306

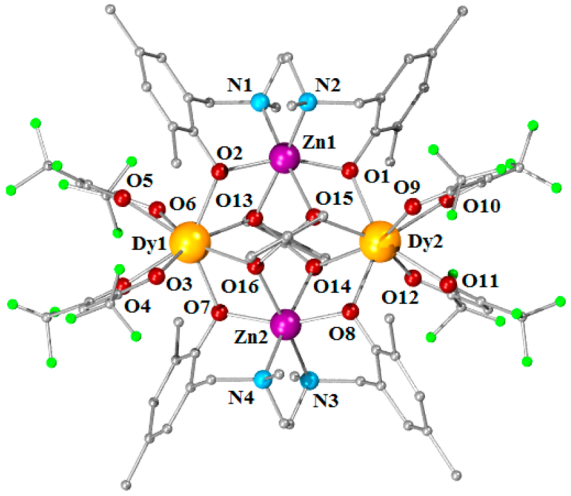

Figure 4. Partially labeled POV-Ray (in ball and stick form) diagram showing the atom-labeling scheme for the complex **6**.

marginal influence on the overall structure. The Zn centers are both octahedral, while the Dy centers are eight-coordinated, providing bicapped trigonal prismatic environments with different degrees of distortions. The Zn···Dy separations are in the range of 3.600−3.640 Å, and the Zn···Dy···Zn (~82°) and Dy···Zn···Dy (~98°) angles are again complementary to each other.

Magnetic Properties. The temperature dependence of magnetic susceptibilities for the isostructural complexes **1**−**6** have been measured on crushed microcrystalline samples over the temperature range of 1.8−300 K using **B** = 0.1 T as the external magnetic field. The plots of dimensionless product function $\chi_{mol}T/C_0$ versus T, where the Curie constant $C_0 = N_A\mu_0\mu_B^2/k_B = 4.7\,141\,997 \times 10^{-6}$ m^3 K mol^{-1}, are displayed in Figures 5A−8A, while the corresponding field-dependent isothermal magnetization studies are shown in Figures 5B−8B.

The basic experimental magnetic data for complexes **1**−**6** are summarized in Table 2. The complex $[Co^{II}_2(L)_2(PhCOO)_2La^{III}_2(hfac)_4]$ **5** behaves magnetically as a $[d^7,d^7]$ dyad with S_{Co} = 3/2. As shown in the inset of Figure 5A, the χ_{mol} versus T

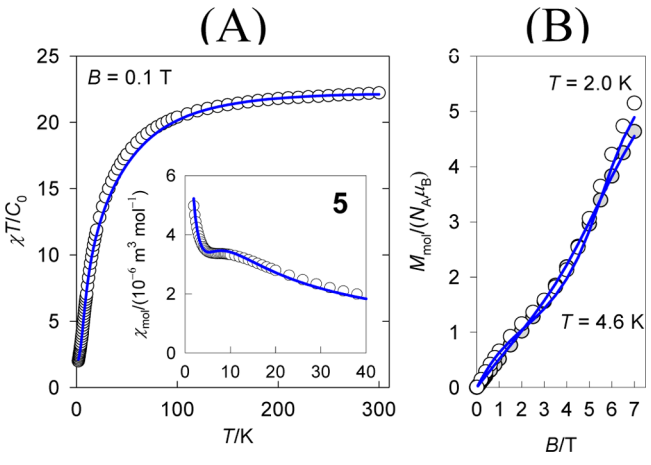

Figure 5. Magnetic functions for complex **5** $[Co^{II}_2La^{III}_2]$. (A) Temperature dependence of the dimensionless product function $\chi T/C_0$; inset: molar magnetic susceptibility in SI units. (B) Field dependence of the magnetization per formula unit. Lines: fitted data (details are in the text).

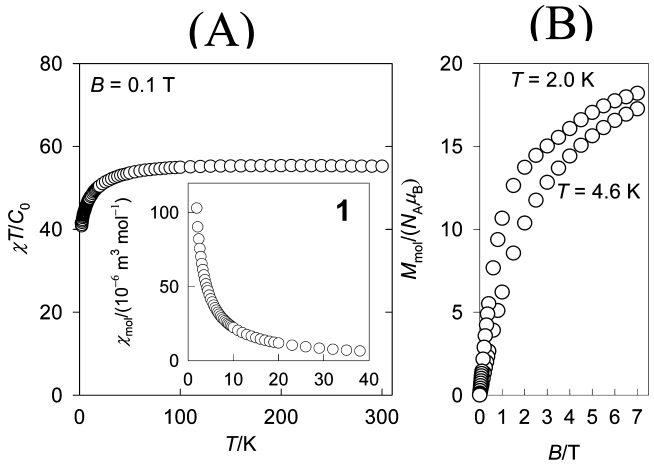

Figure 6. Magnetic functions for the complex **1**, $[Co^{II}_2Gd^{III}_2]$. (A): temperature dependence of the dimensionless product function $\chi T/C_0$; inset: molar magnetic susceptibility; (B): field dependence of the magnetization per formula unit.

plot of this compound gets rounded at the maximum at about 10 K due to antiferromagnetic interaction and then increases continually with further lowering of temperature due to paramagnetic impurity. The value of $\chi_{mol}T/C_0$ at 300 K is 22.2 and can be accounted for only if a high value of g_{Co} = 3 is used in the high-temperature limit expression $\chi T/C_0 = 2 \times g_{Co}^2 S_{Co}(S_{Co}+1)/3 = 22.5$. We emphasize that this rather high value of g_{Co} be accepted as an experimental fact irrespective of the model. It may be noted that although the value of saturation magnetization per formula unit ($M_1 = M_{mol}/N_A\mu_B = 2g_{Co}S_{Co}$) is expected to be 9.0, the observed values at low temperatures indicate the presence of paramagnetic impurity (Figure 5B).

The susceptibility and magnetization data sets have been fitted simultaneously by applying an error functional consisting of relative errors for susceptibility and magnetization $F = R(\chi) \times R(M)$, and details of the model are described in the Supporting Information.[20,21] An advanced optimization routine that utilizes a genetic algorithm converged to the following set of magnetic parameters: $J_{Co-Co}/hc = -5.61$ cm^{-1}, $g_{Co,z} = 2.54$, $g_{Co,x} = 3.31$, $D_{Co}/hc = 62.7$ cm^{-1}; molecular field correction $(zj)/hc = -0.134$ cm^{-1}; temperature independent magnetism $\chi_{TIM} = -9.0 \times 10^{-9}$ m^3 mol^{-1}, mole fraction of the paramagnetic impurity $x_{PI} = 0.066$ [discrepancy factors $R(\chi) = 0.026$ and $R(M) = 0.046$]. The value of the D-parameter lies at the lower edge of D-values reported for hexacoordinate cobalt(II) complexes.[22] The misalignment of the local D-tensors was essential for a successful fit of both the susceptibility and the magnetization data. Note that the geometry of the chromophore *cis*-$[CoN_2(O_{phenoxo})_2(O_{carboxylato})_2]$ is distorted (C_1 symmetry), with the average bond lengths being Co−N = 2.163 Å and Co−$O_{phenoxo}$ = 2.272 Å, and the $O_{phenoxo}$−Co−$O_{phenoxo}$ angles deviate much from 180°, thus producing a rather weak crystal field. A weak crystal field leads to collapsing of the excited crystal field terms and enhances their contribution to the g-factors. Indeed, a modeling shows that $g_x \geq 3$ occurs for a weak crystal field in hexacoordinate Co(II) complexes.[23] Attempts to involve the orbital angular momentum in the spin−orbital basis set explicitly as reported elsewhere[24] has failed in this case.

In the complex $[Co^{II}_2(L)_2(PhCOO)_2Gd^{III}_2(hfac)_4]$ **1**, the magnetically isotropic Gd^{III} ion possesses the $^8S_{7/2}$ ground state. In this case, the high-temperature limit for the dimensionless

dx.doi.org/10.1021/ic401484d | Inorg. Chem. 2014, 53, 1295−1306

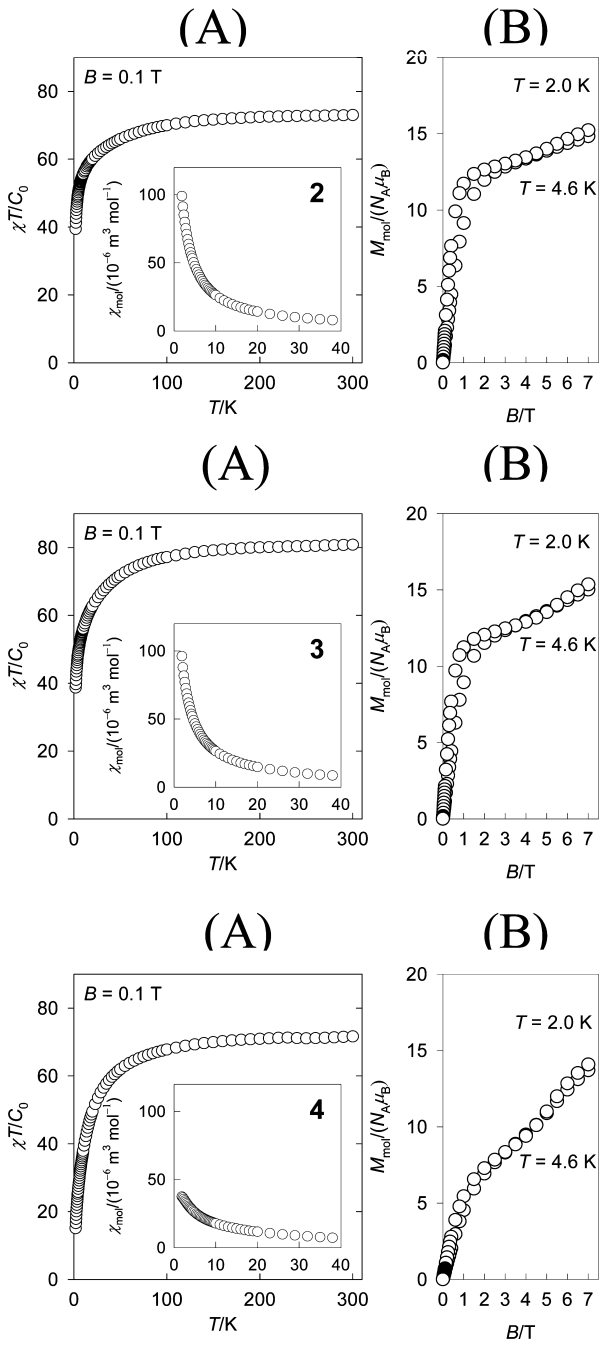

Figure 7. (A): $\chi T/C_0$ vs T plots (inset: molar magnetic susceptibility vs T plots). (B) Field dependence of isothermal magnetization for compounds **2**, **3**, and **4**.

product $\chi T/C_0 = 2g_{Co}{}^2S_{Co}(S_{Co}+1)/3 + 2g_{Co}{}^2S_{Gd}(S_{Gd}+1)/3$ is 52 if both g_{Gd} and $g_{Co} = 2.0$. A bit higher experimental value of 55.2 (Figure 6A) is consistent with $g_{Co} = 2.3$. Again, as may be seen in Figure 6B, the expected value of saturation magnetization ($M_1 = 2g_{Co}S_{Co}+2g_{Gd}S_{Gd}$) is closely approached ($M_1 = 20$ with $g_{Co} = 2.0$ and $M_1 = 20.9$ with $g_{Co} = 2.3$). The expected zero-field splitting at the Co^{II}-centers causes a reduction of M_1 to <20. (A reliable fitting of magnetic data meets difficulties due to the large dimension of the interaction matrix that is not factored when the single-ion zero-field splitting is involved.)

The susceptibility and magnetization data for the complexes $[Co^{II}{}_2(L)_2(PhCOO)_2Tb^{III}{}_2(hfac)_4]$ **2** and $[Co^{II}{}_2(L)_2(PhCOO)_2Dy^{III}{}_2(hfac)_4]$ **3** show similar trends; a plateau

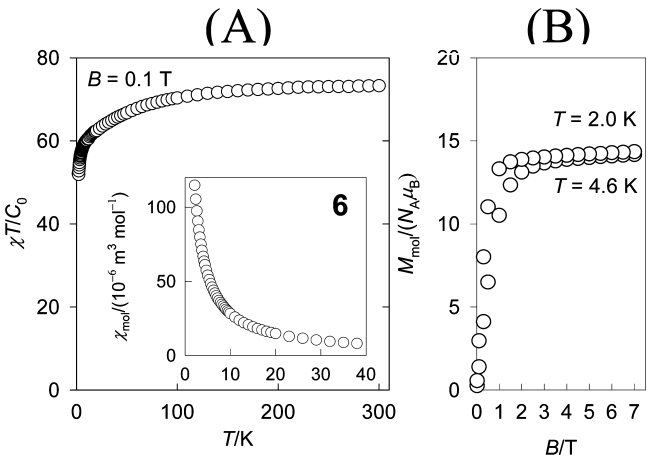

Figure 8. Magnetic functions for complex **6**, $[Zn^{II}{}_2Dy^{III}{}_2]$. (A) Temperature dependence of the dimensionless product function $\chi T/C_0$; inset: molar magnetic susceptibility. (B) Field dependence of the magnetization per formula unit.

exists at the magnetization curve at ca. 3 T (Figure 7). The magnetic behavior of the holmium(III) complex shows some resemblances to **2** or **3**, albeit the plateau of the magnetization curve is less evident in this case and could be due to level crossing. In all these $[d^7,d^7,f^n,f^n]$ tetranuclear systems, the single-ion ground multiplets and the g-factors of the lanthanides are $^7F_6$ and $g_J = 3/2$ for Tb^{III}, $^6H_{15/2}$ and $g_J = 4/3$ for Dy^{III}, and $^5I_8$ and $g_J = 5/4$ for Ho^{III} (ref 20). Using $g_{Co} = 2.0$ in the equation $(\chi T/C_0)_{HT} = 2g_{Co}{}^2S_{Co}(S_{Co}+1)/3 + 2g_J{}^2J_{max}(J_{max}+1)/3$, the calculated and observed values of $\chi T/C_0$ at 300 K are: 73 and 73 for complex **2**, 85.6 and 80.8 for complex **3**, and 85.0 and 71.6 for complex **4**. As will be seen, complexes **2** and **4** do not show a slow magnetic relaxation process as the out-of-phase AC magnetic susceptibility remains silent up to 2 K for each of these compounds.

Compound $[Zn^{II}{}_2(L)_2(PhCOO)_2Dy^{III}{}_2(hfac)_4]$ **6** behaves as a $[f^9,f^9]$ dyad (Figure 8). In the case of Dy^{III} ion, the first excited multiplet ($J = 11/2$) is 4125 cm^{-1} above the ground multiplet ($J_{max} = 15/2$). The calculated high-temperature limit $(\chi T/C_0)_{HT}$ value of 75.5 compares well with the observed room temperature value of 73.2. It may be pointed out that the χT data could indicate antiferromagnetic coupling between $j_1 = j_2 = 15/2$ angular momenta, giving rise to the $J = 0$ ground state. However, the absence of a maximum in the susceptibility curve up to 1.9 K indicates that even in case of such exchange interaction, the coupling constant should be extremely small.

In the model under consideration, the magnetization per formula unit should saturate to $M_1 = 2g_{Dy}J_{max} = 20.0$; however, the observed saturation value at **B** = 7 T and $T = 2.0$ K is only $M_1 = 14.3$. Clearly, this is a fingerprint of an additional level splitting of the J multiplets. As the magnetization grows with the magnetic field very rapidly, a high magnetic anisotropy is expected. This complex did not show any remnant magnetization. The zero-field-cooling magnetization/field-cooling magnetization curves measured at **B** = 5, 10, and 50 mT coincided and thus confirmed the absence of long-range ordering. (Their course is identical with the temperature evolution of the DC-magnetic susceptibility.) The magnetic behavior of complex **6** appears to be analogous to that reported recently in the literature of $[Dy^{III}{}_2Co^{III}{}_2(OMe)_2(teaH)_2(O_2CPh)_4(MeOH)_4](NO_3)_2{\cdot}MeOH{\cdot}H_2O$ and $[Dy^{III}{}_2Co^{III}{}_2(OMe)_2(teaH)_2(O_2CPh)_4(MeOH)_2(NO_3)_2]{\cdot}MeOH{\cdot}H_2O$

dx.doi.org/10.1021/ic401484d | Inorg. Chem. 2014, 53, 1295−1306

Table 2. Key Magnetic Data for the Complexes 1−6

complex, $[M^{II}_2Ln^{III}_2]$	ground multiplet of Ln^{III}	g_J	$(\chi T/C_0)_{HT}$[a]	$(\chi T/C_0)_{300\ K}$	$M_{mol}/(N_A\mu_B)$ at T = 2.0 K, **B** = 7.0 T	$M_{mol}/(N_A\mu_B)$, expected saturation[b]
1 $[Co^{II}_2Gd^{III}_2]$	$^8S_{7/2}$	2	52.0	55.2	18.2	20
2 $[Co^{II}_2Tb^{III}_2]$	$^7F_6$	3/2	73.0	73.0	15.2	24
3 $[Co^{II}_2Dy^{III}_2]$	$^6H_{15/2}$	4/3	85.6	80.8	15.4	26
4 $[Co^{II}_2Ho^{III}_2]$	$^5I_8$	5/4	85.0	71.6	14.1	26
5 $[Co^{II}_2La^{III}_2]$	$^1S_0$	g_{Co} = 3.0	22.5	22.2	5.15	6
6 $[Zn^{II}_2Dy^{III}_2]$	$^6H_{15/2}$	4/3	75.5	73.2	14.3	20

[a]High-temperature estimate using g_{Co} = 2 in the equation $(\chi T/C_0)_{HT} = 2g_{Co}{}^2S_{Co}(S_{Co} + 1)/3 + 2g_J{}^2J_{max}(J_{max} + 1)/3$. [b]Using g_{Co} = 2 in $(M_{mol}/N_A\mu_B)_{sat} = 2g_{Co}S_{Co} + 2g_JJ_{max}$.

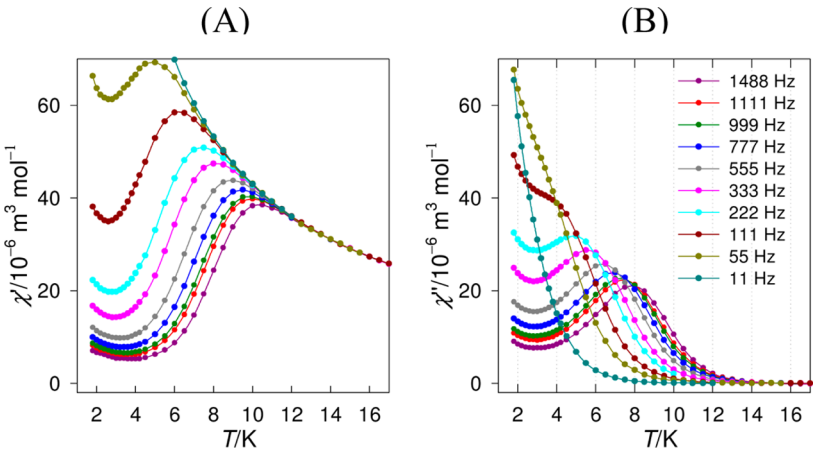

Figure 9. The AC susceptibility data for complex **6** at zero DC field. (A) Temperature dependence of the in-phase molar susceptibility. (B) Temperature dependence of the out-of-phase molar susceptibility (SI units).

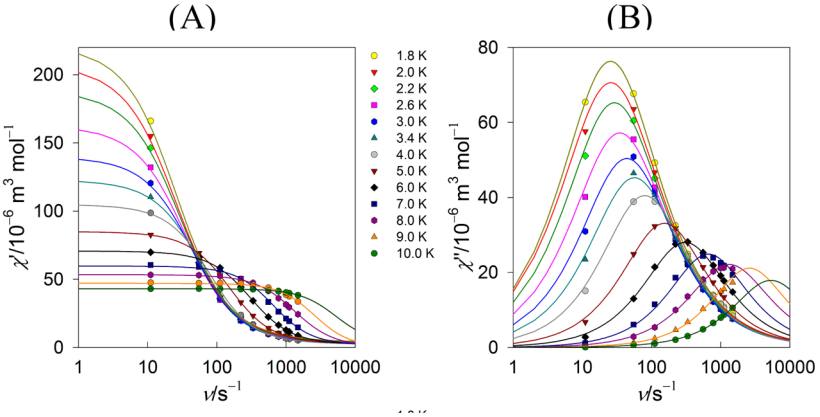

Figure 10. The AC susceptibility data for complex **6** at zero DC field. (A) Frequency dependence of the in-phase molar susceptibility. (B) Frequency dependence of the out-of-phase molar susceptibility. Lines fitted.

($teaH_3$ = triethanolamine).[25] Here the decrease of the χT function on cooling has been attributed to depopulation of M_J sublevels of the ground J state and/or high magnetic anisotropy. The quantum-chemical calculations confirmed that the ground state is a nonmagnetic doublet, while the first excited doublet state lying above at ca. 1.5 cm^{-1} possesses strong magnetic anisotropy (g_z = 39).

To probe the presence of slow magnetic relaxation, compound **6** was further subjected to AC susceptibility measurements. As shown in Figure 9, the compound exhibits a maximum at the out-of-phase susceptibility curve at 8 K (ν = 1500 Hz). As the compound is cooled further, the χ'' component does not fall to the zero, but after reaching a minimum at ca. 3 K, it tends to increase. With the lowering of the frequency of the AC field, the maximum shifts to lower temperatures, which confirms a superparamagnetic behavior and the single-molecule magnetism. However, for frequencies below 111 Hz, the two curves interfere, and at ν = 11 Hz only one component is visible.

The frequency dependence of the complex susceptibility has been fitted according to the well-known Cole−Cole equation $\hat{\chi}(\omega) = \chi_S + (\chi_T - \chi_S)/[1 + (i\omega\tau)^{1-\alpha}]$, where adiabatic ($\chi_S$) and isothermal ($\chi_T$) susceptibilities are related, along with the relaxation time τ and the distribution parameter α ($\omega = 2\pi\nu$). This equation decomposes for the two components, and the fitting procedure was based upon minimization of the error functional $F = R(\chi') \times R(\chi'')$ constructed of the relative errors for the real and imaginary component of the susceptibility. The

dx.doi.org/10.1021/ic401484d | Inorg. Chem. 2014, 53, 1295−1306

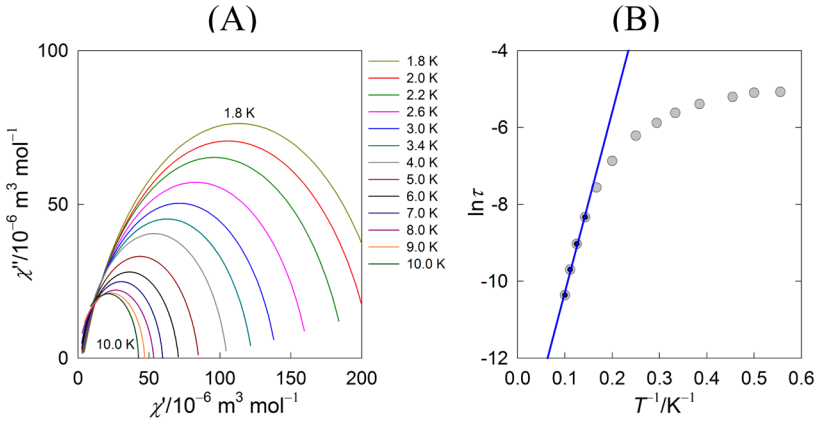

Figure 11. The AC susceptibility data for complex **6** at zero DC field. (A) Cole−Cole plot with fitted lines for fixed temperature. (B) Arrhenius-like fit of ln $\tau = \ln(1/2\pi\nu''_{max})$ vs $1/T$; $U/k_B = 47.9$ K, $\tau_0 = 2.75 \times 10^{-7}$ s.

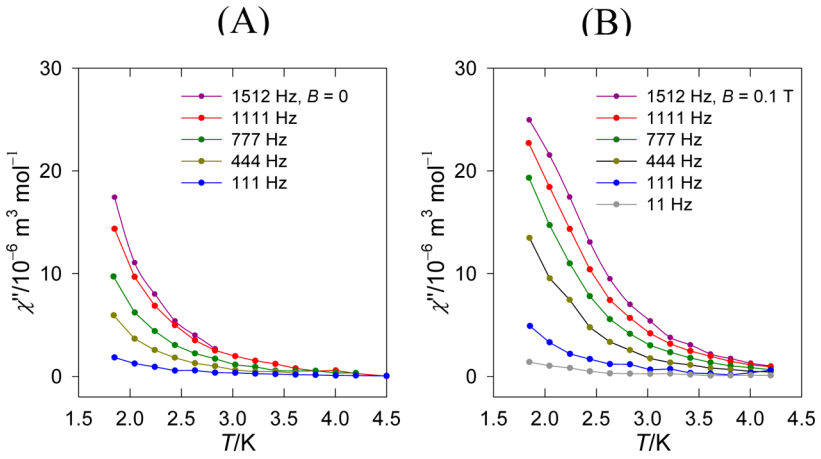

Figure 12. The out-of-phase molar susceptibility χ'' (SI units) for complex **3** at (A) zero and (B) applied DC field. Lines serve as a guide.

results are displayed in Figure 10 for a number of temperatures (T = 1.8−10 K). The resulting parameters were used to generate prediction (solid) lines encompassing interpolation and extrapolation regions. The parameters for individual temperatures are listed (Table S2, Supporting Information).

The data in the worksheets of Figure 10 have been used to generate the Cole−Cole (Argand) diagram as depicted in Figure 11A. The frequency for which $\chi''(\omega)$ adopts a maximum is used in the Arrhenius-like plot ln $\tau = (1/2\pi\nu''_{max})$ vs $1/T$ shown in Figure 11B. The first four points were used for a linear fit, giving rise to the SMM parameters: $U/k_B = 47.9$ K and $\tau_0 = 2.75 \times 10^{-7}$ s. The parameters are typical for single-molecule magnets and are close to those reported for a trinuclear $[Cu^{II}Dy^{III}_2]$ compound.[26] The remaining points in Figure 11B indicate that the thermal activation process starts to alter to the temperature-independent tunneling process of spin reversal. As the distribution parameter α increases on the lowering of temperature, it may be concluded that solid-state defects and disorders play prominent roles at low temperature and adversely affect the admixing of states and hence adversely affect the tunneling rate.

The AC susceptibility measurements were performed also for the $[Co^{II}_2Dy^{III}_2]$ complex **3**. The results indicate that the out-of-phase component χ'' starts to rise below 6 K (Figure 12). The profile of the susceptibility curve depends upon the frequency of the alternating field (ν = 1512, 1111, 777, 444, 111, and 11 Hz) and rises with the applied external field of $\mathbf{B}_{DC}$ = 0.1 T. The expected maximum, however, lies outside the temperature and frequency limits of the standard SQUID setup (T_{min} = 1.8 K, ν_{max} = 1500 Hz). The shift of χ'', however, is well observed and thus confirmed superparamagnetic behavior of complex **3**. A linear plot according to the Arrhenius-like equation $\ln(\chi''/\chi') = \ln(2\pi\nu\tau_0) + U/k_BT$ serves for the estimation of the energy barrier of the single-molecule magnet behavior (Figure 13): $U/k_B \approx 8$ K and $\tau_0 \approx 10^{-7}$ s. This procedure is valid only when $\alpha = 0$, which is true when $\mathbf{B}_{DC} = 0$ (see below). At $\mathbf{B}_{DC}$ = 0.1 T, a deviation from the linearity caused by $\alpha > 0$ is evident.

The AC susceptibility data for complex **3** (at varying frequency) were fitted in the same way as they were for complex **6**, and then Figures 14 and 15 were generated. (Analogous graphs at $\mathbf{B}_{DC} = 0$ are deposited in the Supporting Information, Figures S5 and S6.) It can be concluded that at $\mathbf{B}_{DC}$ = 0.1 T, the distribution parameter ranges as $0.14 < \alpha < 0.20$, as opposed to the case of $\mathbf{B}_{DC} = 0$, when $\alpha \approx 0$ holds true (see Tables S3 and S4, Supporting Information). Consequently, the Cole−Cole plot for complex **3** at $\mathbf{B}_{DC}$ = 0.1 T is represented by flattened arcs (Figure 15A) as against the case of $\mathbf{B}_{DC} = 0$ when it is given by almost perfect semicircles, indicating a single relaxation process. The nonzero value of the adiabatic susceptibility χ_S, as it results from the fitting procedure, causes the arcs and semicircles to merge at high frequencies.

dx.doi.org/10.1021/ic401484d | Inorg. Chem. 2014, 53, 1295−1306

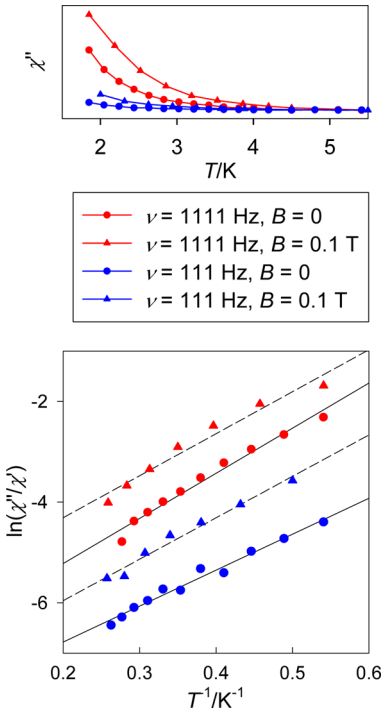

Figure 13. Approximate expression for the slow relaxation according to $\ln(\chi''/\chi') = \ln(2\pi\nu\tau_0) + U/k_BT$ for complex **3** at different frequencies and applied DC field.

The Arrhenius plots for complex **3** are pretty linear ($T > 1.85$ K) for both $\mathbf{B}_{DC} = 0$ and 0.1 T, as shown in the Supporting Information, Figure S6 and in Figure 15B, respectively. This indicates that the thermal activation process is operative exclusively. The Arrhenius plots allow extraction of the SMM parameters: $U/k_B = 8.8$ K ($\tau_0 = 2.0 \times 10^{-7}$ s) at $\mathbf{B}_{DC} = 0$, and $U/k_B = 7.8$ K ($\tau_0 = 3.9 \times 10^{-7}$ s) at $\mathbf{B}_{DC} = 0.1$ T. These values span the range of SMM parameters for Dy^{III}-containing complexes, as documented in Table 3. More examples of Dy^{III} complexes showing SMM behavior can be found in a recent review.[27]

In complex **3**, application of magnetic field $\mathbf{B}_{DC}$ removes the degeneracy of the energy levels to the opposite sides of the barrier. Consequently, the quantum tunneling mechanism can be reduced. This also causes a shift of frequency maxima at $\chi''(T,\nu)$ to higher temperature and lower frequencies so that in some cases the maxima can appear within the hardware capabilities. (Sometimes, however, the applied field moves ν''_{max} to higher values.)[8d]

The observation of the SMM behavior for complex **6** [$Zn^{II}_2Dy_2$], possessing only a pair of magnetoactive Dy(III) ions showing no ferromagnetic exchange coupling, appears to be a paradox. Several examples have been reported so far; for instance, the pure [Dy_2][28] complex and the [$Co^{III}_2Dy_2$][25] system where quite high barriers for spin reversal exist: U/k_B = 76 and 89 K, respectively. The height of the barrier clearly does not correlate with the number of Dy(III) centers in the complex, as documented by the data in Table 3.[29−42] The involvement of atoms with high magnetic anisotropy, like Ni(II) and Co(II), leads to unpredictable changes in the U values. In the [Dy_4] series, the involvement of the heteroatom (diamagnetic or paramagnetic) usually leads to a decrease of U.[8f,29−37] Thus, the important question of why the substitution of two Zn(II) centers in complex **6** for Co(II) ones in complex **3** causes an acceleration (still slow) of magnetic relaxation remains unanswered. Some recent reports suggest that the embodiment of paramagnetic metal centers such as Cr(III) in the [M_2Dy_2] core can enhance the blocking temperature through 3d magnetic exchange.[43] However, this is not generally true as documented by comparison of our complexes **3** and **6**.

CONCLUSIONS

In summary, a series of [2 × 2] 3d−4f heterometal complexes of cobalt(II) and lanthanide(III) ions (Ln^{III} = Gd, Tb, Dy, Ho, and La) have been reported along with an analogous [$Zn^{II}_2Dy^{III}_2$] compound. Structurally these compounds are unique in that the metal centers are all connected by carboxylato bridges in a rare μ_4–η^2:η^2 mode. The lanthanide centers in these complexes are surrounded by eight oxygen donors, generating a bicapped pseudotrigonal prismatic coordination environment, while the cobalt centers have a distorted octahedral geometry. The compounds are all isostructural, exhibiting paramagnetic behavior with no remnant DC-magnetization detected for them. The metal centers in these heterometallic complexes are coupled in an antiferromagnetic manner. Quenching of the orbital contribution in the case of Co^{II}, induced by significant distortions from the ideal octahedron geometry, is prevalent in these complexes. A slow

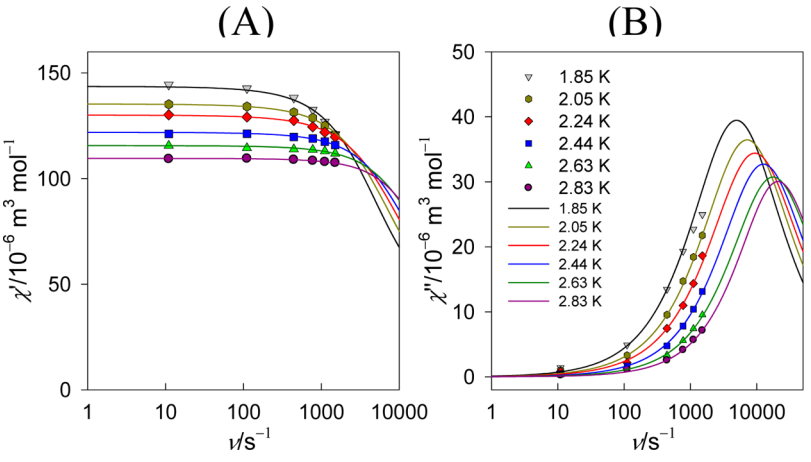

Figure 14. The AC susceptibility data for complex **3** at $\mathbf{B}_{DC} = 0.1$ T. (A) Frequency dependence of the in-phase molar susceptibility. (B) Frequency dependence of the out-of-phase molar susceptibility. Lines fitted.

dx.doi.org/10.1021/ic401484d | Inorg. Chem. 2014, 53, 1295−1306

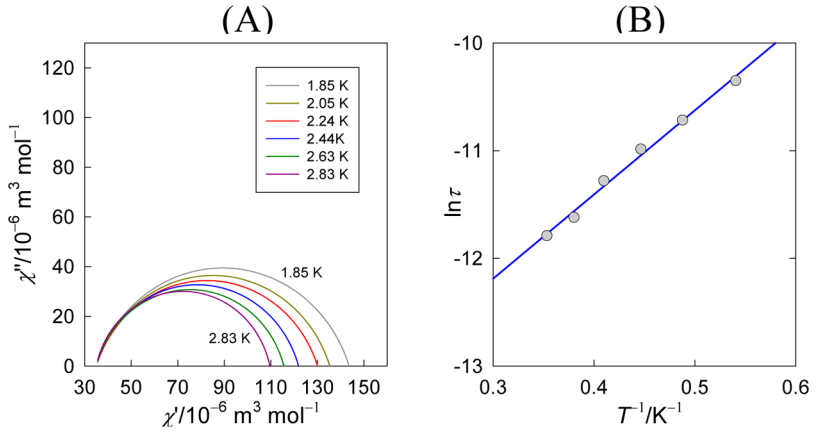

Figure 15. The AC susceptibility data for complex **3** at B_{DC} = 0.1 T. (A) Cole–Cole plot with fitted lines for fixed temperature. (B) Arrhenius-like fit of ln τ = ln$(1/2\pi f''_{max})$ vs $1/T$; U/k_B = 7.81 K, $\tau_0 = 3.9 \times 10^{-7}$ s.

Table 3. Selected Examples of Dy-Containing Single Molecule Magnets

complex of Dy^{III}	B_{DC}/T	(U/k_B)/K[a]	τ_0/s	α	ref.
[Dy]	0.1	46.1[b]	6.4×10^{-6}	0.02–0.09	42
[Dy]	0.1	36.5[b]	7.9×10^{-7}	0.01–0.07	42
[Dy]	0.1	49.3[b]	4.8×10^{-6}	0.05–0.10	42
[Dy]	0.1	37.0[b]	7.7×10^{-7}	0.01–0.07	42
[Dy]	0.1	30.5	1.1×10^{-7}	0.04–0.05	42
[Dy]	0.1	25.1	4.0×10^{-7}	0.06–0.07	42
[Y^{III}Dy]	0.2	17.3	1.52×10^{-7}		41
[Fe^{III}Dy]	0	8.98	7.77×10^{-8}		7c
[Co^{II}_2Dy]	0	14.2	5.1×10^{-6}		8a
[Co^{II}_6Dy]	0	n.a.	n.a.		8i
[Dy_2]	0	76	6×10^{-7}	0.03–0.18	28
[$Cu^{II}Dy_2$]	0	47	1×10^{-7}		26
[$Co^{III}_2Dy_2$]	0	88.8	5.64×10^{-8}	0.24–0.29	25
6, [$Zn^{II}_2Dy_2$]	0	47.9	2.75×10^{-7}	0.08–0.17	this Work
[$Co^{II}_2Dy_2$]	0	82.1[b]	6.2×10^{-7}	0.005–0.045	8h
[$Co^{II}_2Dy_2$]		11.0[b]	7.7×10^{-4}		8h
3, [$Co^{II}_2Dy_2$]	0	8.8 (ext)	2.0×10^{-7}	0.00–0.07	this Work
3, [$Co^{II}_2Dy_2$]	0.1	7.8 (ext)	3.9×10^{-7}	0.14–0.20	this Work
[$Ni^{II}_2Dy_2$]	0.075	13.6	7.7×10^{-8}	0.16–0.24	39
[$Ni^{II}_2Dy_2$]$_\infty$[1]	0.1	17.4	7.7×10^{-7}	0.10–0.30	39
[$Cu^{II}_8Dy_3$]	0	n.a.	n.a.		35
[Dy_4]	0.18	110	6.5×10^{-7}		36
[Dy_4]		91	4.5×10^{-7}		37
[Dy_4]	0	54.2[b]	7.2×10^{-7}	0.09–0.18	34
[Dy_4]		16.8[b]	1.4×10^{-6}	0.41–0.58	34
[Dy_4]		23	8×10^{-8}		30
[Dy_4]	0	5.4	1.1×10^{-5}		33
[$Co^{III}_2Dy_4$]	0.06	3.8	4.8×10^{-6}		32
[$Co^{III}_2Dy_4$]	0	2 (est)	10^{-6} (est)		29
[$Co^{II}_4Dy_4$]	0, 0.2	n.a.	n.a.		31
[$Co^{II}_2Co^{III}_4Dy_4$]	0	n.a.	n.a.		8f
[$Co^{II}_{11}Dy_6$]	0, 0.2	n.a.	n.a.		31
[$Mn^{II}_2Mn^{III}_2Dy_6$]	0	n.a.	n.a.		40
[Dy_8]	0, 0.15	n.a.	n.a.		38
[Dy_{10}]	0, 0.15	n.a.	n.a.		38
[$Co^{II}_2Dy_{10}$]	0	25[b]	3.14×10^{-6}	0.18–0.20	8d
[$Co^{II}_2Dy_{10}$]		4.3[b]	1.13×10^{-4}		8d

[a]Est–estimated via $\ln(\chi''/\chi') = \ln(2\pi\nu\tau_0) + U/k_BT$; ext–based mostly upon extrapolation; n.a.–not available because the frequency maxima lie below the limits of the hardware (1.8 K). [b]Two relaxation processes.

magnetic relaxation has been confirmed by AC susceptibility measurements for the [$Co^{II}_2Dy^{III}_2$] and [$Zn^{II}_2Dy^{III}_2$] compounds, showing a single-molecule magnet behavior. In the complex [$Zn^{II}_2Dy^{III}_2$], the SMM parameters are U/k_B = 47.9 K

dx.doi.org/10.1021/ic401484d | Inorg. Chem. 2014, 53, 1295–1306

($\tau_0 = 2.75 \times 10^{-7}$ s); whereas, in the complex [$Co^{II}_2Dy^{III}_2$], the reduction of the barrier to spin reversal and a faster (still slow) magnetic relaxation were detected: $U/k_B = 8.8$ K ($\tau_0 = 2.0 \times 10^{-7}$ s) at $\mathbf{B}_{DC} = 0$, and $U/k_B = 7.8$ K ($\tau_0 = 3.9 \times 10^{-7}$ s) at $\mathbf{B}_{DC} = 0.1$. The presence of a highly anisotropic Dy^{III} ion is largely responsible for the existence of such energy barrier for spin reversal in compounds **3** and **6**, leading to their SMM-type behavior.

■ ASSOCIATED CONTENT

Supporting Information

Skeletal view of the core structure of compound **1** (Figure S1), Persistence of Vision Raytracer (POV-Ray) diagrams for the complexes **2**, **3**, and **4** (Figures S2−4), selected metrical parameters for complexes **1**−**6** (Table S1), SMM parameters for complexes **3** and **6** (Tables S2−4 and Figures S5 and S6) and X-ray crystallographic files in CIF format for compounds **1**−**6**. This material is available free of charge via the Internet at http://pubs.acs.org.

■ AUTHOR INFORMATION

Corresponding Authors

*E-mail: icmc@iacs.res.in. (M.C.)
*E-mail: roman.boca@stuba.sk. (R.B.)

Notes

The authors declare no competing financial interest.

■ ACKNOWLEDGMENTS

We thank Professor K. Nag for many helpful discussions. This work was supported by the Council of Scientific and Industrial Research (CSIR), New Delhi. Three of us (S.M.T.A., M.C.M., and M.M.) also thank the CSIR for the award of Research Fellowships. The single-crystal X-ray diffraction data were recorded on an instrument supported by DST, New Delhi, as a National Facility at IACS under the IRHPA program. Grant Agencies (Slovakia: VEGA 1/0522/14 and 1/0233/12, APVV-0014-11) are also acknowledged for the financial support.

■ REFERENCES

(1) (a) Sessoli, R.; Powell, A. K. *Coord. Chem. Rev.* **2009**, *253*, 2328. (b) Andruh, M. *Chem. Commun.* **2007**, 2565. (c) Sorace, L.; Benelli, C.; Gatteschi, D. *Chem. Soc. Rev.* **2011**, *40*, 3092.

(2) Bencini, A.; Benelli, C.; Caneschi, A.; Carlin, R. L.; Dei, A.; Gatteschi, D. *J. Am. Chem. Soc.* **1985**, *107*, 8128.

(3) See, for example: (a) Luzon, J.; Bernot, K.; Hewitt, I. J.; Anson, C. E.; Powell, A. K.; Sessoli, R. *Phys. Rev. Lett.* **2008**, *100*, 24720. (b) Chibotaru, L. F.; Ungur, L.; Soneini, A. *Angew. Chem., Int. Ed.* **2008**, *47*, 4126. (c) Lin, P.-H.; Burchell, T. J.; Clérac, R.; Murugesu, M. *Angew. Chem., Int. Ed.* **2008**, *47*, 8848. (d) Ishikawa, N.; Sugita, M.; Ishikawa, T.; Koshihara, S.; Kaizu, Y. *J. Am. Chem. Soc.* **2003**, *125*, 8694.

(4) (a) Wernsdorfer, W.; Aliaga-Alcade, N.; Hendrickson, D. N.; Christou, G. *Nature* **2002**, *416*, 406. (b) Leuenberger, M. N.; Loss, D. *Nature* **2001**, *410*, 789. (c) Ritter, S. K. *Chem. Eng. News* **2004**, *82*, 29. (d) Sessoli, R.; Gatteschi, D.; Caneschi, A.; Novak, M. *Nature* **1993**, *365*, 141. (e) Inglis, R.; Jones, L. F.; Karotsis, G.; Collins, A.; Parsons, S.; Perlepes, S. P.; Wernsdorfer, W.; Brechin, E. K. *Chem. Commun.* **2008**, 5924. (f) Maheswaran, S.; Chastanet, G.; Teat, S. J.; Mallah, T.; Sessoli, R.; Wernsdorfer, W.; Winpenny, R. E. P. *Angew. Chem., Int. Ed.* **2005**, *44*, 5044. (g) Binnemans, K.; Galyametdinov, Y. G.; Van Deun, R.; Bruce, D. W.; Collinson, S. R.; Polishchuk, A. P.; Bikchantaev, I.; Haase, W.; Prosvirin, A. V.; Tinchurina, L.; Litvinov, U.; Gubajdullin, A.; Rakhmatullin, A.; Uytterhoeven, K.; Van Meervelt, L. *J. Am. Chem. Soc.* **2000**, *122*, 4335. (h) Gschneidner, K. A., Jr.; Pecharsky, V. K. L. *J. Appl. Phys.* **1999**, *85*, 5365.

(5) (a) Novitchi, G.; Wernsdorfer, W.; Chibotaru, L. F.; Costes, J. P.; Anson, C. E.; Powell, A. K. *Angew. Chem., Int. Ed.* **2009**, *48*, 1614. (b) Novitchi, G.; Costes, J. P.; Tuchagues, J. P.; Vendier, L.; Wernsdorfer, W. *New J. Chem.* **2008**, *32*, 197. (c) Kajiwara, T.; Takahashi, K.; Hiraizumi, T.; Takaishi, S.; Yamashita, M. *CrystEngComm* **2009**, *11*, 2110. (d) Kajiwara, T.; Nakano, M.; Takaishi, S.; Yamashita, M. *Inorg. Chem.* **2008**, *47*, 8604. (e) Baskar, V.; Gopal, K.; Helliwell, M.; Tuna, F.; Wernsdorfer, W.; Winpenny, R. E. P. *Dalton Trans.* **2010**, *39*, 4747. (f) Costes, J.-P.; Dahan, F.; Wernsdorfer, W. *Inorg. Chem.* **2006**, *45*, 5. (g) Osa, S.; Kido, T.; Matsumoto, N.; Re, N.; Pochaba, A.; Mrozinski, J. *J. Am. Chem. Soc.* **2004**, *126*, 420. (h) Costes, J.-P.; Vendier, L.; Wernsdorfer, W. *Dalton Trans.* **2010**, *39*, 4886. (i) Aronica, C.; Pilet, G.; Chastanet, G.; Wernsdorfer, W.; Jacquot, J. F.; Luneau, D. *Angew. Chem., Int. Ed.* **2006**, *45*, 4659. (j) Aronica, C.; Chastanet, G.; Pilet, G.; Le Guennic, B.; Robert, V.; Wernsdorfer, W.; Luneau, D. *Inorg. Chem.* **2007**, *46*, 6108. (k) Okazawa, A.; Nogami, T.; Nojiri, H.; Ishida, T. *Chem. Mater.* **2008**, *20*, 3110. (l) Okazawa, A.; Nogami, T.; Nojiri, H.; Ishida, T. *Inorg. Chem.* **2008**, *47*, 9763. (m) Okazawa, A.; Nogami, T.; Nojiri, H.; Ishida, T. *Inorg. Chem.* **2009**, *48*, 3292. (n) Iasco, O.; Novitchi, G.; Jeanneau, E.; Wernsdorfer, W.; Luneau, D. *Inorg. Chem.* **2013**, *52*, 8723.

(6) (a) Zaleski, C. M.; Kampf, J. W.; Mallah, T.; Kirk, M. L.; Pecoraro, V. L. *Inorg. Chem.* **2007**, *46*, 1954. (b) Zaleski, C. M.; Depperman, E. C.; Kampf, J. W.; Kirk, M. L.; Pecoraro, V. L. *Angew. Chem., Int. Ed.* **2004**, *43*, 3912. (c) Stamatatos, T. C.; Teat, S. J.; Wernsdorfer, W.; Christou, G. *Angew. Chem., Int. Ed.* **2009**, *48*, 521. (d) Mereacre, V.; Ako, A. M.; Clérac, R.; Wernsdorfer, W.; Hewitt, I. J.; Anson, C. E.; Powell, A. K. *Chem.—Eur. J.* **2008**, *14*, 3577. (e) Mishra, A.; Wernsdorfer, W.; Parsons, S.; Christou, G.; Brechin, E. K. *Chem. Commun.* **2005**, 2086. (f) Mishra, A.; Tasiopoulos, A. J.; Wernsdorfer, W.; Moushi, E. E.; Moulton, B.; Zaworotko, M. J.; Abboud, K. A.; Christou, G. *Inorg. Chem.* **2008**, *47*, 4832.

(7) (a) Akhtar, M. N.; Mereacre, V.; Novitchi, G.; Tuchagues, J.-P.; Anson, C. E.; Powell, A. K. *Chem.—Eur. J.* **2009**, *15*, 7278. (b) Abbas, G.; Lan, Y.; Mereacre, V.; Wernsdorfer, W.; Clérac, R.; Buth, G.; Sougrati, M. T.; Grandjean, F.; Long, G. J.; Anson, C. E.; Powell, A. K. *Inorg. Chem.* **2009**, *48*, 9345. (c) Ferbinteanu, M.; Kajiwara, T.; Choi, K. Y.; Nojiri, H.; Nakamoto, A.; Kojima, N.; Cimpoesu, F.; Fujimura, Y.; Takaishi, S.; Yamashita, M. *J. Am. Chem. Soc.* **2006**, *128*, 9008.

(8) (a) Pineda, E. M.; Tuna, F.; Pritchard, R. G.; Regan, A. C.; Winpenny, R. E. P.; McInnes, E. J. L. *Chem. Commun.* **2013**, *49*, 3522. (b) Zheng, Y.-Z.; Evangelisti, M.; Tuna, F.; Winpenny, R. E. P. *J. Am. Chem. Soc.* **2012**, *134*, 1057. (c) Zheng, Y.-Z.; Evangelisti, M.; Winpenny, R. E. P. *Chem. Sci.* **2011**, *2*, 99. (d) Chandrasekhar, V.; Pandian, B. M.; Vittal, J. J.; Clérac, R. *Inorg. Chem.* **2009**, *48*, 1148. (e) Costes, J.-P.; Vendier, L.; Wernsdorfer, W. *Dalton Trans.* **2011**, *40*, 1700. (f) Yamaguchi, T.; Costes, J.-P.; Kishima, Y.; Kojima, M.; Sunatsuki, Y.; Brefuel, N.; Tuchagues, J.-P.; Vendier, L.; Wernsdorfer, W. *Inorg. Chem.* **2010**, *49*, 9125. (g) Zou, L.-F.; Zhao, L.; Guo, Y.-N.; Yu, G.-M.; Guo, Y.; Tang, J.; Li, Y.-H. *Chem. Commun.* **2011**, *47*, 8659. (h) Zhao, X. Q.; Lan, Y. H.; Zhao, B.; Cheng, P.; Anson, C. E.; Powell, A. K. *Dalton Trans.* **2010**, *39*, 4911. (i) Xiang, H.; Lan, Y. H.; Li, H. Y.; Jiang, L.; Lu, T. B.; Anson, C. E.; Powell, A. K. *Dalton Trans.* **2010**, *39*, 4737. (j) Gómez, V.; Vendier, L.; Corbella, M.; Costes, J.-P. *Inorg. Chem.* **2012**, *51*, 6396. (k) Mondal, K. C.; Sundt, A.; Lan, Y.; Kostakis, G. E.; Waldmann, O.; Ungur, L.; Chibotaru, L. F.; Anson, C. E.; Powell, A. K. *Angew. Chem., Int. Ed.* **2012**, *51*, 7550. (l) Sopasis, G. J.; Orfanoudaki, M.; Zarmpas, P.; Philippidis, A.; Siczek, M.; Lis, T.; O'Brien, J. R.; Milios, C. J. *Inorg. Chem.* **2012**, *51*, 1170. (m) Towatari, M.; Nishi, K.; Fujinami, T.; Matsumoto, N.; Sunatsuki, Y.; Kojima, M.; Mochida, N.; Ishida, T.; Re, N.; Mrozinski, J. *Inorg. Chem.* **2013**, *52*, 6160. (n) Costes, J. P.; Dahan, F.; Garcìa-Tojal, J. *Chem.—Eur. J.* **2002**, *8*, 5430.

(9) (a) Mandal, D. Ph.D. Thesis, Jadavpur University, Kolkata, India, 2007. (b) Mandal, D.; Chatterjee, P. B.; Ganguly, R.; Tiekink, E. R. T.; Clérac, R.; Chaudhury, M. *Inorg. Chem.* **2008**, *47*, 584.

(10) Richardson, M. F.; Wagner, W. F.; Sands, D. E. *J. Inorg. Nucl. Chem.* **1968**, *30*, 1275.

(11) Perrin, D. D.; Armarego, W. L. F.; Perrin, D. R. *Purification of Laboratory Chemicals*, 2nd ed.; Pergamon: Oxford, 1980.
(12) *SADABS (version 2.03)*; Bruker AXS Inc.: Madison, WI, 2002.
(13) Sheldrick, G. M. *Acta Crystallogr.* **1990**, *46A*, 467.
(14) Sheldrick, G. M. *SHELXL−97, Program for Crystal Structure Refinements*; University of Göttingen: Germany, 1996.
(15) *SAINT (version 6.02)*; Bruker AXS, Inc.: Madison, WI, 2002.
(16) *DIAMOND, Visual Crystal Structure Information System, version 3.1*; Crystal Impact: Bonn, Germany, 2004.
(17) (a) Chandler, C.; Fallon, G. D.; West, B. O. *J. Chem. Soc., Chem. Commun.* **1990**, 1063. (b) Mikuriya, M.; Tanaka, K.; Inoue, N.; Yoshioka, D.; Lim, J.-W. *Chem. Lett.* **2003**, *32*, 126.
(18) Nakamoto, K. *Infrared and Raman Spectra of Inorganic and Coordination Compounds*, 3rd ed.; Wiley-Interscience: New York, 1978.
(19) (a) Kido, T.; Ikuta, Y.; Sunatsuki, Y.; Ogawa, Y.; Matsumoto, N. *Inorg. Chem.* **2003**, *42*, 398. (b) Yamaguchi, T.; Sunatsuki, Y.; Ishida, H.; Kojima, M.; Akashi, H.; Re, N.; Matsumoto, N.; Pochaba, A.; Mroziński, J. *Inorg. Chem.* **2008**, *47*, 5736.
(20) Hudák, J.; Boča, R.; Moncol, J.; Titiš, J. *Inorg. Chim. Acta* **2013**, *394*, 401.
(21) Boča, R. *A Handbook of Magnetochemical Formulae*; Elsevier: Amsterdam, 2012.
(22) (a) Titiš, J.; Boča, R. *Inorg. Chem.* **2011**, *50*, 11838. (b) Hudák, J.; Boča, R.; Dlháň, L.; Kožíšek, J.; Moncol, J. *Polyhedron* **2011**, *30*, 1367.
(23) Boča, R. *Struct. Bonding (Berlin, Ger.)* **2006**, *117*, 1.
(24) Ostrovsky, S. M.; Falk, K.; Pelikan, J.; Brown, D. A.; Tomkowicz, Z.; Haase, W. *Inorg. Chem.* **2006**, *45*, 688.
(25) Langley, S. K.; Chilton, N. F.; Ungur, L.; Moubaraki, B.; Chibotaru, L. F.; Murray, K. S. *Inorg. Chem.* **2012**, *51*, 11873.
(26) Mori, F.; Nyui, T.; Ishida, T.; Nogami, T.; Choi, K.-Y.; Nojiri, H. *J. Am. Chem. Soc.* **2006**, *128*, 1440.
(27) Woodruff, D. N.; Winpenny, R. E. P.; Layfield, R. A. *Chem. Rev.* **2013**, *113*, 5110.
(28) Long, J.; Habib, F.; Lin, P.-H.; Korobkov, I.; Enright, G.; Ungur, L.; Wernsdorfer, W.; Chibotaru, L. F.; Murugesu, M. *J. Am. Chem. Soc.* **2011**, *133*, 5319.
(29) Jhan, S.-Y.; Huang, S.-H.; Yang, C.-I; Tsai, H.-L. *Polyhedron* **2013**, *66*, 222.
(30) Lin, P.-H.; Korobkov, I.; Wernsdorfer, W.; Ungur, L.; Chibotaru, L. F.; Murugesu, M. *Eur. J. Inorg. Chem.* **2011**, 1535.
(31) Langley, S. K.; Chilton, N. F.; Moubaraki, B.; Murray, K. S. *Polyhedron* **2013**, *66*, 48.
(32) Feuersenger, J.; Prodius, D.; Mereacre, V.; Clérac, R.; Anson, C. E.; Powell, A. K. *Polyhedron* **2013**, *66*, 257.
(33) Abbas, G.; Kostakis, G. E.; Lan, Y.; Powell, A. K. *Polyhedron* **2012**, *41*, 1.
(34) Chandrasekhar, V.; Hossain, S.; Das, S.; Biswas, S.; Sutter, J.-P. *Inorg. Chem.* **2013**, *52*, 6346.
(35) Iasco, O.; Novitchi, G.; Jeanneau, E.; Luneau, D. *Inorg. Chem.* **2013**, *52*, 8723.
(36) Randell, N. M.; Anwar, M. U.; Drover, M. W.; Dawe, L. N.; Thompson, L. K. *Inorg. Chem.* **2013**, *52*, 6731.
(37) Anwar, M. U.; Thompson, L. K.; Dawe, L. N.; Habib, F.; Murugesu, M. *Chem. Commun.* **2012**, *48*, 4576.
(38) Langley, S. K.; Moubaraki, B.; Murray, K. S. *Polyhedron* **2013**, *64*, 255.
(39) Pasatoiu, T. D.; Etienne, M.; Madalan, A. M.; Andruh, M.; Sessoli, R. *Dalton Trans.* **2010**, *39*, 4802.
(40) Majeed, Z.; Mondal, K. C.; Kostakis, G. E.; Lan, Y.; Anson, C. E.; Powell, A. K. *Dalton Trans.* **2010**, *39*, 4740.
(41) Kan, J.; Wang, H.; Sun, W.; Cao, W.; Tao, J.; Jiang, J. *Inorg. Chem* **2013**, *52*, 8505.
(42) Liu, C.-M.; Zhang, D.-Q.; Zhu, D.-B. *Inorg. Chem* **2013**, *52*, 8933.
(43) Langley, S. K.; Vielechowski, D. P.; Vieru, V.; Chilton, N. F.; Moubaraki, B.; Abrahams, B. F.; Chibotaru, L. F.; Murray, K. S. *Angew. Chem., Int. Ed.* **2013**, *52*, 12014.